Chaotic Advection in a Three-Dimensional Stokes Flow

A. J. S. Rodrigo and J. P. B. Mota
Dept. de Química, Centro de Química Fina e Biotecnologia, Faculdade de Ciências e Tecnologia, Universidade Nova de Lisboa, 2829-516 Caparica, Portugal

A. Lefevre, J. C. Leprévost, and E. Saatdjian
CNRS GDR 681: Chaos Lagrangien 3-D, 2 ave. de la forêt de Haye, BP 160, 54504 Vandoeuvre Cédex, France

Mixing by chaotic advection is studied in a new 3-D flow geometry. It consists of two confocal elliptic cylinders whose inner and outer boundaries glide circumferentially so that the geometry does not vary with time. Dye advection experiments have been performed and compared to numerical streak lines calculated using the analytical solution of Stokes' equations in elliptical cylindrical coordinates. Experiments show that particle trajectories remain for all practical purposes inside tubes defined by the potential mixing zone during the whole process. For the case where the elliptic cylinders turn time periodically in opposite directions, we examine the effect of the modulation frequency of the boundary displacement protocol by defining appropriate dimensionless control parameters and then numerically monitoring the advection of a passive scalar. It is shown that for a given average axial velocity, there is an optimum modulation frequency that maximizes the mixing enhancement due to chaotic advection.

Introduction

Chaotic advection in devices where fluid flows in tubes of uniform cross section is an interesting alternative to static mixers when a substance is to be blended into a very viscous fluid. In some important industrial cases, the transport and mixing of highly viscous fluids through a static mixer leads to pressure drops that are so high that the process becomes economically unfeasible. The earliest mathematical work on chaotic advection was performed by Poincaré and appears in his work on celestial mechanics (Poincaré, 1893). However, it was the article by Aref (1984) on a blinking vortex flow that has sparked the recent interest on the subject.

Chaotic particle trajectories are possible in both periodic two-dimensional (2-D) flows and in three-dimensional (3-D) flows (Ottino, 1989). However, most numerical and experimental studies are concerned with 2-D periodic systems; in other words, with batch mixing. For the journal-bearing flow, a configuration that has been widely studied both theoretically and experimentally, Chaiken et al. (1986) and Swanson and Ottino (1990) have constructed a rotating eccentric cylinder apparatus to visualize streamlines when the two cylinders turn at constant angular velocities, and to study chaotic advection when the boundaries are displaced either one at a time or with angular velocities that vary periodically in time.

Several tools have been developed to study mixing in these flows. The starting point, whenever it is available, is the analytical solution of Stokes' equations (inertial effects are not important when the Reynolds number is below unity, as is the case here and in the literature cited) for constant boundary conditions. When the boundary motion is time-periodic, the analytical solution at the instantaneous values of the boundary velocities is assumed to hold. This assumption is only valid when both the Reynolds and the Strouhal numbers are small. For this pseudo−steady flow, dye advection experiments can be compared successfully with numerical simulations based on the analytical solution. Poincaré sections can be plotted easily for 2-D flows. A Poincaré section tells if a given location in the flow is regular or chaotic (for the given boundary displacement protocol). However, Poincaré sections do not give any indication on the mixing rate. Other quantities that can be calculated using the steady-state flow field are the periodic points, the stretching field (Swanson

Correspondence concerning this article should be addressed to E. Saatdjian.

and Ottino, 1990), and the analogous heat-transfer rate (Ghosh et al., 1992). In conjunction, all these tools provide the engineer with a method to optimize somewhat the mixing process, apparatus, and boundary displacement protocol.

A similar flow concerns fluid between two confocal elliptic cylinders that glide circumferentially so that the geometry remains invariant. The equations of motion can be written in elliptical cylindrical coordinates that are orthogonal and similar to bipolar coordinates. However, unlike bipolar coordinates, elliptical coordinates do degenerate into cylindrical coordinates as the eccentricity of the inner ellipse tends toward unity (or the focal radius tends toward zero). The analytical solution of Stokes' equations in elliptical coordinates has been obtained by Saatdjian et al. (1994).

An elliptic mixer working on this principle has been constructed by Saatdjian et al. (1996). Although the apparatus is more complicated to build and operate than the eccentric cylinder system, it possesses two main advantages as far as mixing is concerned. The first advantage is that this geometry possesses two symmetry axis instead of one [see, for example, Franjione et al. (1989)]. The second advantage is topological, the steady counterrotating case exhibits two saddle points in the regions of minimum gap. Thus, by their disruption, fluid is allowed from one closed region into another at two different locations, so one can expect twice as much gain (from chaotic advection), as in the journal-bearing flow. Another point is that the counterrotating case becomes more chaotic as the eccentricity of the inner ellipse is increased without increasing the size of the regular region. This is not the case in the journal-bearing flow, where a compromise must be found between eccentricity (here the distance between the centers of the cylinders) and the size of regular islands in the region of maximum gap, as shown in Aref and Balachandar (1986). In a theoretical study on the journal-bearing flow, Kaper and Wiggins (1993) conclude that the best boundary displacement protocol is one where the angular velocity ratio varies over the widest range for a very small value of the eccentricity.

However, industry is often interested in continuous mixing and not in batch processes. Although some theoretical and numerical work is available on several three-equation chaotic dynamical systems, such as the Lorenz equations or the ABC flows (which are highly simplified models of fluid flow in particular situations), there are not many chaotic advection studies in 3-D open flows that have been constructed experimentally. Two exceptions are the twisted-pipe flow, which has been studied by Jones et al. (1989), Acharya et al. (1992), and Peerhossaini et al. (1993), and the partitioned-pipe mixer (Khakhar et al., 1987). In the twisted-pipe flow, chaotic trajectories are created by primary and secondary Dean vortices in the curved and twisted geometry. However, as in static mixers, there is no control parameter, and a closed-form analytical solution valid for all cases is not known. To improve the mixing process, one must change the geometry of the tube, for example, by increasing the number of bends or by modifying the static mixer length.

If an axial velocity component is superimposed onto the eccentric cylinder system, the flow becomes 3-D, and is known as the eccentric helical annular mixer (EHAM). In this case, one can control the mixing process by varying the displacements of both cylinders. An apparatus that does precisely this was constructed by Kusch and Ottino (1992) and experimental streak lines were compared to numerical results obtained using the analytical solution of the 3-D Stokes equations. In 3-D flows there are just a few analytical or numerical tools that can be used to optimize this process (for example, Poincaré sections are of practically no use and give very little information since they are time periodic; a given location can be chaotic or regular, depending on the time instant) and much work is yet to be done on this issue.

In this article, we first describe a new experimental setup that we have constructed for 3-D mixing studies. It consists of two confocal elliptic cylinders with axial flow. Both the inner and outer boundaries can be displaced circumferentially time periodically. As has been shown previously, although more difficult to build, this flow geometry should be more effective for mixing than the EHAM. Dye advection experiments are performed and compared with success to numerical streak lines. We then look at the important problem of optimizing the boundary displacement protocol. We first define two dimensionless control parameters obtained by scaling the cross-sectional velocity protocol with respect to the mean residence time in the mixer. We then study how fluid with nonuniform distribution of a passive scalar behaves inside the mixer. For a given geometry we show that an appropriate choice of the two control parameters leads to a more effective mixing.

The Flow Between Confocal Elliptic Cylinders

The 3-D analytical solution of the equations of motion in elliptical cylindrical coordinates and for constant velocities of both boundaries is given in this section. Consider two vertical, confocal elliptic cylinders (Figure 1 shows the cross-section). Elliptical, cylindrical coordinates $[u, v, z]$ are defined by the following transformations

$$x = a \cosh u \cos v, \qquad y = a \sinh u \sin v, \qquad z = z$$

where a is the focal radius. This coordinate system is orthogonal, and the metric coefficients in the three directions $[h_u, h_v, h_z]$ are

$$h_u = h_v = h = a\sqrt{\cosh^2 u - \cos^2 v}, \qquad h_z = 1$$

As shown in Figure 1, the inner and outer ellipses are defined by the curves $u = u_1$ and $u = u_2$, respectively.

Both the inner and outer walls can *glide circumferentially* at a prescribed velocity. Notice that the geometry does not vary with time. The equations of motion for an incompressible, Newtonian fluid when inertia is negligible are

$$\nabla \cdot \boldsymbol{V} = 0, \qquad \nabla P = \mu \nabla^2 \boldsymbol{V}$$

where μ is the fluid dynamic viscosity.

Since the two tangential velocity components $[hV_u, hV_v]$ can be obtained independently from the axial flow, it is obvious that the axial velocity component V_z is independent of the axial coordinate z, that is

$$\frac{\partial V_z}{\partial z} = 0$$

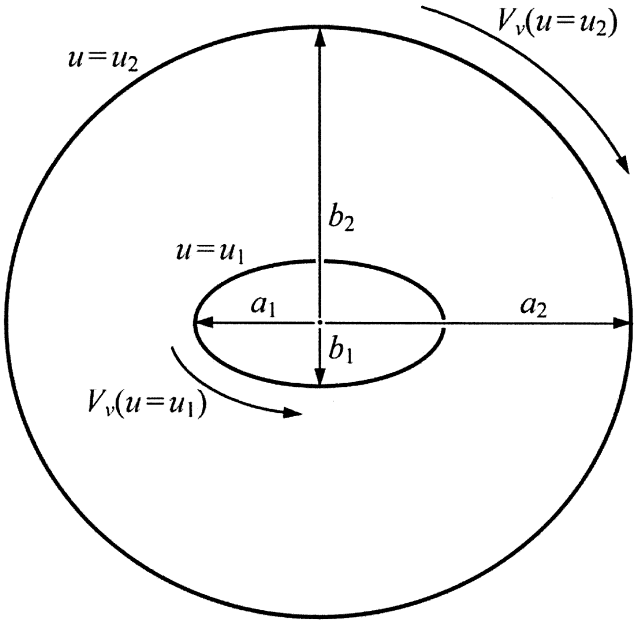

Figure 1. Cross-sectional area of 3-D mixer and elliptical cylindrical coordinates notation.

The confocality condition sets a relationship between the axis of the outer ellipse, $b_2/a_2 = 1 - s(1+\sqrt{1-s})^{-1}$, where $s = (a_1/a_2)^2[1-(b_1/a_1)^2]$.

In this case, the axial component of the equations of motion

$$\frac{h^2}{\mu}\frac{\partial P}{\partial z} = \frac{\partial^2 V_z}{\partial u^2} + \frac{\partial^2 V_z}{\partial v^2}$$

can be solved independently of the other two components. It is for this reason that this flow is said to be $2\frac{1}{2}$-D by some researchers. Its solution is obtained using the separation-of-variables technique, it is

$$V_z(u,v) = \frac{a^2}{8\mu}\frac{dP}{dz}\left[G_0(u) + G_1(u)\cos 2v\right]$$

where the functions $G_0(u)$ and $G_1(u)$ are

$$G_0(u) = \cosh 2u + \frac{\cosh 2u_1 - \cosh 2u_2}{u_2 - u_1}u + \frac{u_1\cosh 2u_2 - u_2\cosh 2u_1}{u_2 - u_1}$$

and

$$G_1(u) = 1 + \frac{\sinh 2u_1 - \sinh 2u_2}{\sinh 2(u_2 - u_1)}\cosh 2u + \frac{\cosh 2u_2 - \cosh 2u_1}{\sinh 2(u_2 - u_1)}\sinh 2u$$

The two tangential components of the equations of motion were solved previously by Saatdjian et al. (1994), so only a brief summary is given here. If the axial vorticity is labeled ω, and defining a stream function ψ such that

$$hV_u = -\frac{\partial\psi}{\partial v}, \qquad hV_v = \frac{\partial\psi}{\partial u}$$

the two equations can be written in a $\omega-\psi$ formulation as

$$\frac{\partial^2\omega}{\partial u^2} + \frac{\partial^2\omega}{\partial v^2} = 0, \qquad \frac{\partial^2\psi}{\partial u^2} + \frac{\partial^2\psi}{\partial v^2} = h^2\omega$$

The preceding equations can be solved analytically by a Fourier series expansion. The stream function is shown to be of the form

$$\psi = \sum_{n=0}^{\infty} F_n(u)\cos 2nv$$

where

$$F_0(u) = A_0 + B_0u + C_0\cosh 2u + D_0\sinh 2u,$$

$$F_1(u) = A_1\cosh 2u + B_1\sinh 2u + C_0 + C_1\cosh 4u + D_1\sinh 4u,$$

$$F_n(u) = A_n\cosh 2nu + B_n\sinh 2nu + C_{n-1}\cosh 2(n-1)u + D_{n-1}\sinh 2(n-1)u + C_n\cosh 2(n+1)u + D_n\sinh 2(n+1)u + D_n\sinh 2(n+1)u$$

and A_n, B_n, C_n, and D_n are constants determined from the boundary conditions.

With the analytical expressions for the three velocity components one can construct a three-equation dynamical system, which is solved numerically when the boundaries are displaced time periodically. Trajectories of material points, streak lines, and other kinematical tools for the analysis of mixing in this flow geometry can be developed using this analytical solution. In this work, passive tracers were advected in the flow using the DASSL code (Petzold, 1982), which is a variable step-size variable order implementation of the backward differentiation formulas (Gear, 1971).

Experimental Setup

The experimental apparatus is shown in Figure 2. A rectangular casing contains the two gliding confocal ellipses. The experiments are monitored through the view window, which extends from top to bottom on two sides of the rectangular casing. The space between the outer ellipse and the rectangular casing is filled with working fluid in order to reduce optical distortion from the outer ellipse curvature.

The working fluid first enters an input zone, passes across a settling plate, and then flows vertically downwards between the two confocal elliptic cylinders. Once the fluid has flowed through the working section, it goes into a drain tank. The lengths of the minor and major axes of the inner ellipse are,

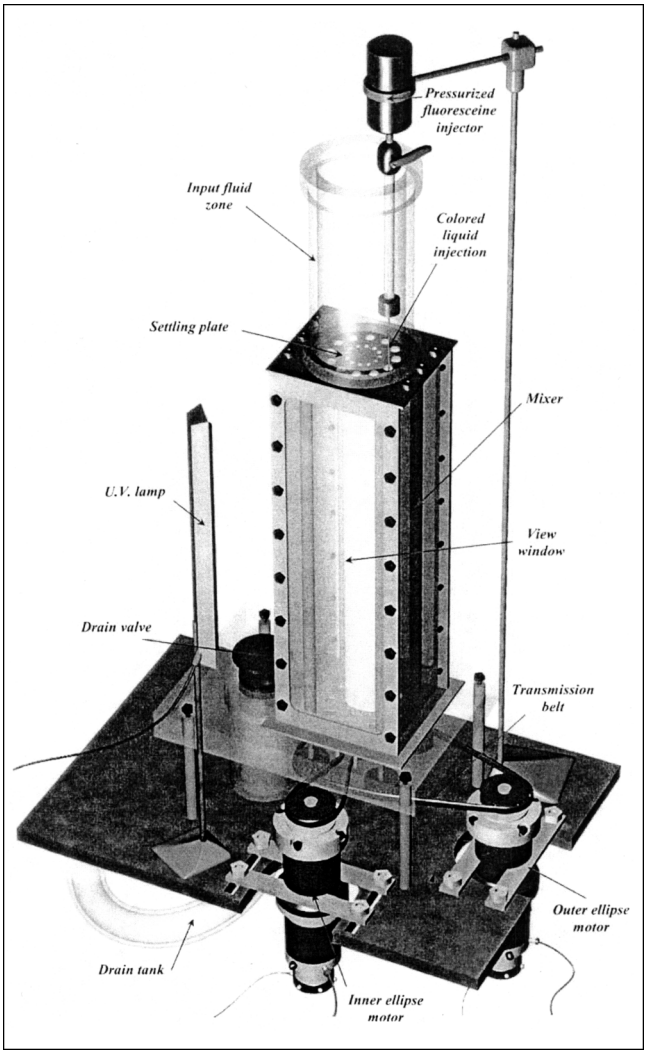

Figure 2. Experimental setup.

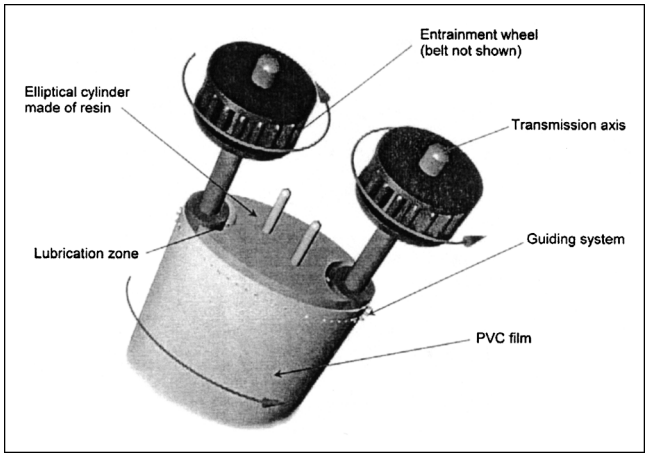

Figure 3. The inner ellipse displacement mechanism.

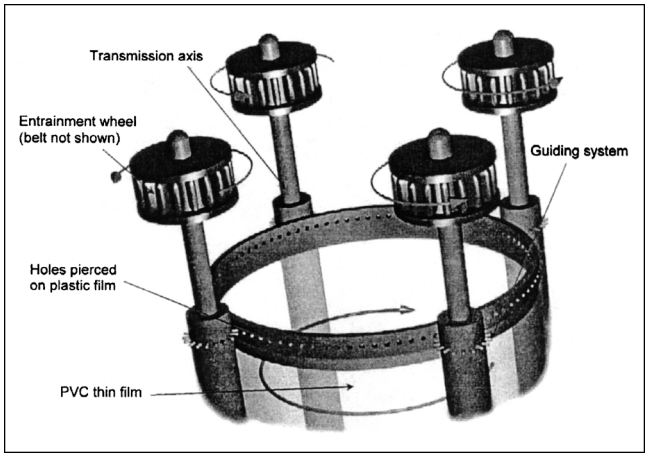

Figure 4. The outer ellipse displacement mechanism.

respectively, $b_1 = 0.02$ m and $a_1 = 0.04$ m. The outer ellipse has a major axis a_2 that is 0.1 m long and the length, $b_2 = 0.938$ m, of its minor axis is imposed by the confocality condition. The axial length of the cylinders is $L = 0.6$ m.

The inner and outer elliptical boundaries are displaced by GEC-Alsthom RTR 60/8 motors, which are fixed to the support block. The displacement of the two motors is monitored via a PC with an ADA 2100 analogical/digital converter. Obviously one of the main difficulties of this apparatus is creating the elliptic motion of the two boundaries. Figure 3 shows the guiding mechanism of the inner ellipse. The inner boundary, a solid elliptic cylinder, has two transmission wheels that are entrained by one motor via a belt. The transmission wheels displace an outer PVC plastic film, which is 2×10^{-4} m thick and is attached to its surface. All moving mechanisms are lubricated with the working fluid.

A sketch of the displacement of the outer boundary is shown in Figure 4. The elliptical boundary displacement is obtained via four transmission wheels, a motor, and a belt. A thin PVC film that is both transparent and resistant covers the outer cylinder. At the top and the bottom of the apparatus, the film was strengthened with a more resistive plastic. It was pierced with small holes in order to make the elliptic guiding motion feasible. This allowed us to perform at least four experiments without breaking the PVC film.

The fluid employed in the experiments is EMKAROX diluted with water so that it behaves like a Newtonian fluid. The fluid density and viscosity are $\rho = 1{,}097$ kg·m^{-3} and $\mu = 6.28$ Pa·s, respectively. The colored fluid was either rhodamine or fluorescein diluted in EMKAROX and water so that the density is the same as the working fluid.

The tracer is injected into the fluid at a specified location in the working zone via a pressurized needle. The average axial velocity or the fluid-average flow rate are controlled by a valve at the exit of the apparatus. Special care was taken to eliminate most of the air bubbles in the viscous fluid. To do this, fluid was continuously fed into the apparatus from a reservoir above it.

The experimental procedure and suggestions described in Kusch and Ottino (1992) were followed here. In particular, the system was run for several minutes until steady-state conditions were obtained. The axial and tangential Reynolds

numbers in our experiments are typically

$$Re_{\text{axial}} = \frac{\rho\langle V_z\rangle(a_2 - a_1)}{\mu} = 0.005$$

$$Re_{\text{tang}} = \frac{\rho(hV_v)|_{u_2}(a_2 - a_1)}{\mu} = 0.1$$

where $\langle V_z\rangle$ is the average axial velocity and $(hV_v)|_{u_2}$ is the tangential velocity of the outer ellipse. These are well within the Stokes flow assumptions. The Strouhal number in the experiments, defined as

$$Sr = \frac{\omega(a_2 - a_1)}{(hV_v)|_{u_2}}$$

where ω is the modulation frequency of the inner ellipse, is typically of the order of $Sr = 0.003$. The experimental setup is also described in Leprévost (2000).

Experimental Results and Discussion

Although it has not yet been stated before, the values of some of the parameters defining this apparatus were chosen using results obtained from a study of the 2-D flow (Saatdjian et al., 1996; Leprévost and Saatdjian, 1998). In particular, the cross-sectional parameters that define this geometry, $a_2/a_1 = 2.5$ and $b_1/a_1 = 0.5$, the direction of motion of the two boundaries (the counterrotating case is the only one considered here), and the time-periodic modulation of the inner ellipse have been assigned values that ensure rapid mixing in the 2-D flow. A compromise in the value of geometrical parameters is nevertheless necessary, because the construction of an ellipse with a very small value of its eccentricity (b_1/a_1) is a major technological difficulty. For the 2-D problem, the counterrotating case is the most interesting one because it contains saddle points. Furthermore, as in the journal-bearing flow, the hyperbolic saddle points are displaced from one boundary to the other when the instantaneous angular velocity ratio changes. It is for this reason that Swanson and Ottino (1990) investigated the 2-D blinking, counterrotating flow. However, in their 3-D EHAM study, Kusch and Ottino (1992) only consider blinking co-rotation. Perhaps this is due to the fact that this boundary displacement exhibits heteroclinic trajectories in the 2-D periodic case.

Figure 5 shows experimental streak lines for the first 5 periods of an experimental run. The important parameters are: $\langle V_z\rangle = 4.5\times10^{-4}$ m/s; the outer boundary is moving at the

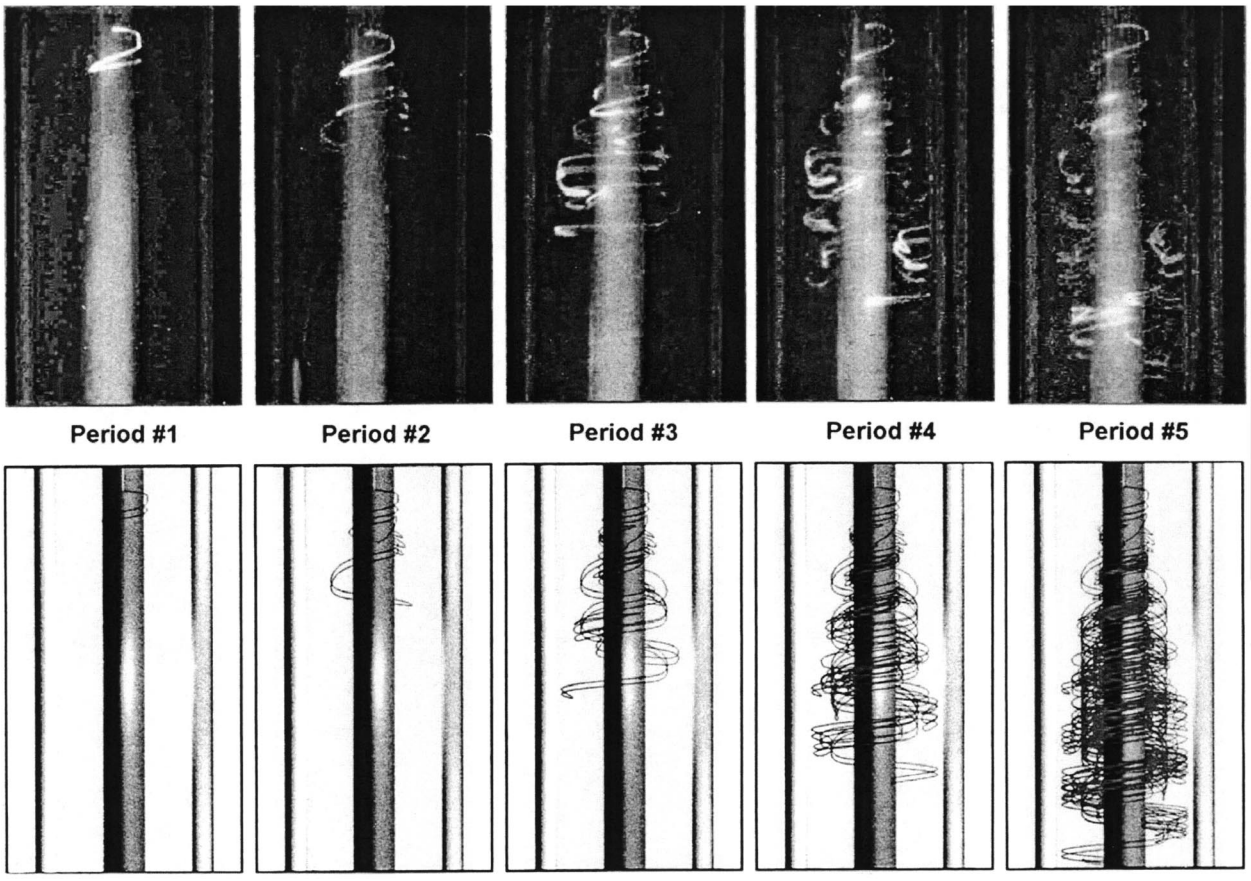

Figure 5. Experimental (top) and numerical (bottom) streak lines for the first 5 periods of a continuous boundary displacement protocol.

The geometric parameters (see Figure 1) are: $a_1 = 0.04$ m, $b_1 = 0.02$ m, $a_2 = 0.1$ m, $L = 0.6$ m; the corresponding cross-sectional geometric ratios are: $a_2/a_1 = 2.5$ and $b_1/a_1 = 0.5$. The inner ellipse turns with a periodic angular velocity defined by Eq. 1; the outer ellipse turns at the constant angular velocity $V_v|_{u_2} = -1$ rpm; the average axial velocity is $\langle V_z\rangle = 4.5\times10^{-3}$ m/s.

constant angular velocity, $V_v|_{u_2} = -1$ rpm, and the inner boundary is turning in the opposite direction with a periodic angular velocity

$$V_v|_{u_1}(t) = 1 + 0.9\cos(\omega t) \text{ rpm}, \qquad \omega = 6 \text{ rad/min} \quad (1)$$

This run is compared to streak lines obtained numerically. The numerical simulation is based on the analytical solution of the 3-D laminar flow with constant boundary conditions. As mentioned earlier, we assume that the flow is pseudosteady.

The agreement between experiment and the numerical simulation is excellent for the first three periods, and it is quite good for the next two. The first five periods of this experiment correspond to a time slightly greater than 5 min. Now, chaos can be defined as sensitivity to initial conditions. So, although much care was taken in adjusting the boundary displacements to their prescribed value and in determining the position of the tracer injection point, there is always an experimental uncertainty. A slight discrepancy between measured and true values will lead, after a certain number of periods, to a big difference in the final result. In this experiment, we have measured (numerically) the length of the streak line after five periods: it is approximately 30 m long.

Another experiment can serve to illustrate the chaotic behavior of this system. The trajectories of particles in the mixer can also be calculated using the dynamical system of three differential equations for this flow. To illustrate this, we use the same geometrical parameters, but a higher value of $\langle V_z \rangle$, in order to reduce the average residence time in the mixer. In this numerical experiment five particles are injected from the same location at intervals of 10^{-3} s. Figure 6 shows different views of this experiment. From the side views, one can see that the particle trajectories start to diverge from one another only after a small axial distance, z, has been covered. The top view also shows the particle trajectories. Although the 3-D periodic flow is not a Hamiltonian system, as is the 2-D periodic flow, some information is common to both systems. If a 3-D trajectory is plotted on a plane, as is done in Figure 6, the tracer will be delimited by approximately the same region as that given by the potential mixing zone defined by Kaper and Wiggins (1993) for the eccentric cylinder system and by Leprévost and Saatdjian (1998) for the confocal elliptic geometry considered here. The tracer trajectory seems to be bounded by vertical tubes and does not move into regular regions near the two boundaries. Simulations with the eccentric cylinder system (Rodrigo et al., 2002) have led to the same result. Unlike most tools available for the periodic 2-D flow (such as Poincaré sections), which are of little use in 3-D flows, the potential mixing zone seems to give information that can be transposed to the 3-D flow. More on this subject is given in the next section when Figure 9 is discussed.

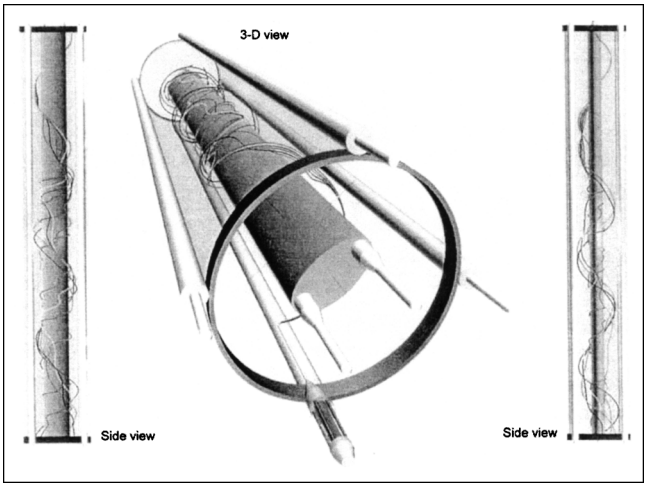

Figure 6. Side and top views of particle trajectory simulations.

The geometric parameters and velocity protocol are identical to those of Figure 5, except for the average axial velocity, which is $\langle V_z \rangle = 10^{-3}$ m/s.

Mixing Enhancement by Time-Periodic Modulation

In this section we look at the fundamental problem of finding a set of optimum operating conditions for our 3-D mixer. In particular, questions that should be ultimately answered are: How should the boundaries be displaced? What is the appropriate value of the average flow rate? What mixer length is required? Obviously, answers to all of these questions must be given before such an apparatus is to be used in a given process. The procedure presented here is derived from a similar analysis that we have made for the EHAM mixer (Rodrigo et al., 2002).

The full optimization of our 3-D mixer, geometry, and operating protocol, is beyond the scope of the present article. However, if some choices (which are not too restrictive) are made first, the task just mentioned becomes feasible here. To begin, the cross-sectional geometry is specified: it is the same as that of our experimental setup. Furthermore, the inner and outer boundaries are assumed to turn in opposite directions (counterrotating case), with the outer cylinder turning at a constant velocity and the inner cylinder turning at a velocity that varies time periodically, as given by Eq. 1. However, here the optimum modulation frequency is yet to be determined, and we examine its effect on the mixing enhancement. Finally, the average angular velocity ratio $V_v|_{u_1}/V_v|_{u_2} = -2$ is fixed. Obviously, a much lower value (for example, -5) would probably lead to better results, since the saddle points (in the 2-D periodic flow) would be displaced over a greater distance. Again, a compromise must be found to place the parametric study within the operating constraints of our experimental apparatus.

To optimize ω, we first define two dimensionless control parameters that scale the boundary displacement with respect to the average residence time $\tau = L/\langle V_z \rangle$ of the fluid in the mixer. The first one is a measure of the number of turns that the cylinder makes per fluid residence time in the mixer. This number is

$$N_T = \frac{V_v|_{u=u_2}\tau}{2\pi}$$

The second one, N_P, defined as

$$N_P = \frac{\omega\tau}{2\pi}$$

is a measure of the number of modulation periods of the inner cylinder per residence time in the mixer. According to the choices just given, N_T is fixed at 30, but N_P has not been assigned a value, because the most appropriate value of the modulation frequency is yet to be determined.

There are several tools or tests that one may perform on the mixer to compare between the efficiency of two distinct mixing protocols. Most theoretical tools for studying mixing, such as Poincaré sections, the stretching distribution of material lines, or simulated blob-deformation experiments, rely on Lagrangian simulations of particle tracking. Although Lagrangian tools possess many advantages (namely, the possibility of addressing the important limit of scalar transport at infinite Péclet number), they are computationally inefficient for a parametric study, because no information can be transposed from one run to another (such as initial guess of the solution). The method adopted here is a numerical experiment consisting of introducing fluid with a nonuniform distribution of a passive scalar into the mixer and monitoring its behavior in an Eulerian framework at high Péclet number. The better protocol is the one that results in a more uniform distribution of the passive scalar at the outlet. Without loss of generality, we take the fluid temperature as the passive scalar. The procedure is described below.

For a given 3-D periodic velocity field, V, obtained analytically, the temperature field inside the mixer is obtained by solving numerically the convection-diffusion equation

$$\frac{\partial T}{\partial t} + V \cdot \nabla T = \alpha \nabla^2 T \tag{2}$$

with adiabatic boundary conditions. Here α is the thermal diffusivity of the fluid. Defining the mixed mean temperature, as usual, at any cross-section and any instant of time as

$$\langle T \rangle = \frac{1}{A\langle V_z \rangle} \int\int_A V_z T dA, \qquad A = \pi(a_2 b_2 - a_1 b_1)$$

the standard deviation σ' of the temperature distribution at the same instant and axial location is

$$(\sigma')^2 = \frac{1}{A\langle V_z \rangle} \int\int_A V_z (T - \langle T \rangle)^2 dA$$

Since this process is time periodic, the standard deviation, at a given axial location, is also time periodic once the steady periodic regime has been reached. Under these conditions, a steady value of σ' can be obtained by averaging σ' over the duration $2\pi/\omega$ of the period of modulation, that is

$$\bar{\sigma}' = \lim_{t \to \infty} \frac{\omega}{2\pi} \int_t^{t + 2\pi/\omega} \sigma' \, dt$$

Finally, we normalize the value of $\bar{\sigma}'$ with respect to the inlet standard deviation σ_0'

$$\bar{\sigma} = \bar{\sigma}'/\sigma_0'$$

All the numerical work presented here was done for an axial Péclet number $Pe = \langle V_z \rangle L/\alpha = 5{,}000$. This value is appropriate for viscous organic liquids such as those considered here. We employed the computational fluid dynamics package FLUENT (version 5.4) for the numerical solution of the 3-D convection–diffusion equation, Eq. 2. The velocity components of the flow field were computed using the analytical solution of the 3-D laminar flow with the pseudo-steady flow assumption. The geometry was mapped to elliptical cylindrical coordinates on a structured grid employing $40 \times 80 \times 50$ (u, v, z) points covering the whole mixer domain. The numerical scheme employs a second-order implicit approximation of the time derivative and second-order upwind discretization with flux correction for the convection terms (Barth and Jespersen, 1989). When applied on an orthogonal grid, such as the one employed here, this differencing scheme is very effective at minimizing numerical diffusion. Preliminary experiments using different grid sizes confirmed this assumption. At each time step, the linearized form of the discretized scalar transport equation was solved using a point-implicit (Gauss-Seidel) linear equation solver in conjunction with an algebraic multigrid method (Hutchinson and Raithby, 1986) to ensure fast convergence.

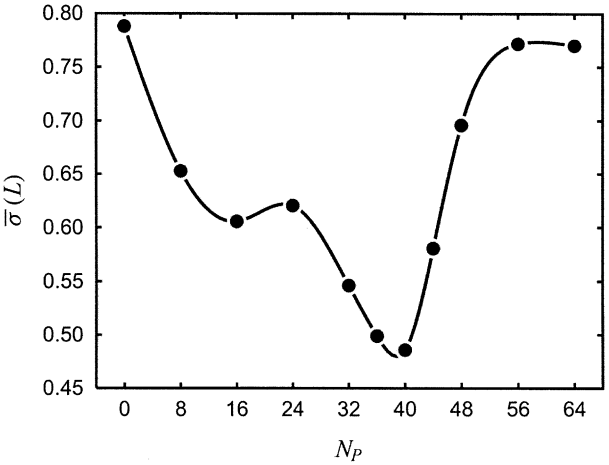

Figure 7. Standard deviation $\bar{\sigma}$ of temperature field at the exit of the mixer, under steady periodic conditions, as a function of the number of modulation periods, N_P, of the inner ellipse.

The cross-sectional geometric parameters (see Figure 1) are: $a_2/a_1 = 2.5$ and $b_1/a_1 = 0.5$. The number of turns of the outer ellipse per residence time in the mixer is $N_T = 30$. The outer ellipse turns at constant angular velocity, while the inner one turns time-periodically in the opposite direction, as given by Eq. 1, with modulation frequency defined by the corresponding value of N_P. The average angular velocity ratio is $\bar{V}_v|_{u_1}/\bar{V}_v|_{u_2} = -2$.

Figure 7 shows the exit value of $\bar{\sigma}$ as a function of N_P for $N_T = 30$. Obviously, the better protocol is the one for which the value of $\bar{\sigma}$ is lower at the exit. Notice that there is a given value of N_P ($N_P = 40$ here) that minimizes the value of $\bar{\sigma}$ at the exit. The presence of an optimum value of the inner cylinder modulation for which mixing is more effective has also been observed in the EHAM mixer (Rodrigo et al., 2002). This result is, in a way, similar to the one obtained by Ghosh et al. (1992) in the 2-D periodic journal-bearing flow. However, in 3-D flows, specifying the value of the modulation frequency is not enough. The value of the average flow rate is

also required. The existence of an optimum modulation frequency that maximizes the enhanced transport in 2-D open cavity flows also has recently been observed by Horner et al. (2002). Overall, these results demonstrate that the mixing rate can be enhanced by properly tuning the modulation frequency of the boundary displacement protocol without any extra effort (per period).

The results of Figure 7 can also be presented by showing the exit temperature distribution using a color code; this is done in Figure 8. For reference, the inlet distribution is shown at the top. The outlet temperature distribution is plotted for four different values of N_P, namely 0, 16, 40, and 64. The plots on the left use the same color code as that of the inlet distribution. The plots on the right are drawn with a narrower color range in order to highlight even further small differences in the temperature distribution. Notice that the exit distribution for $N_P = 0$ is not very different from the one with $N_P = 64$. In both plots, the orange layer near the outer cylinder is quite thick and the end result is not very homogeneous. For $N_P = 16$, and more so for $N_P = 40$, the exit distribution is much more uniform and the orange layer near the outer wall is thinner.

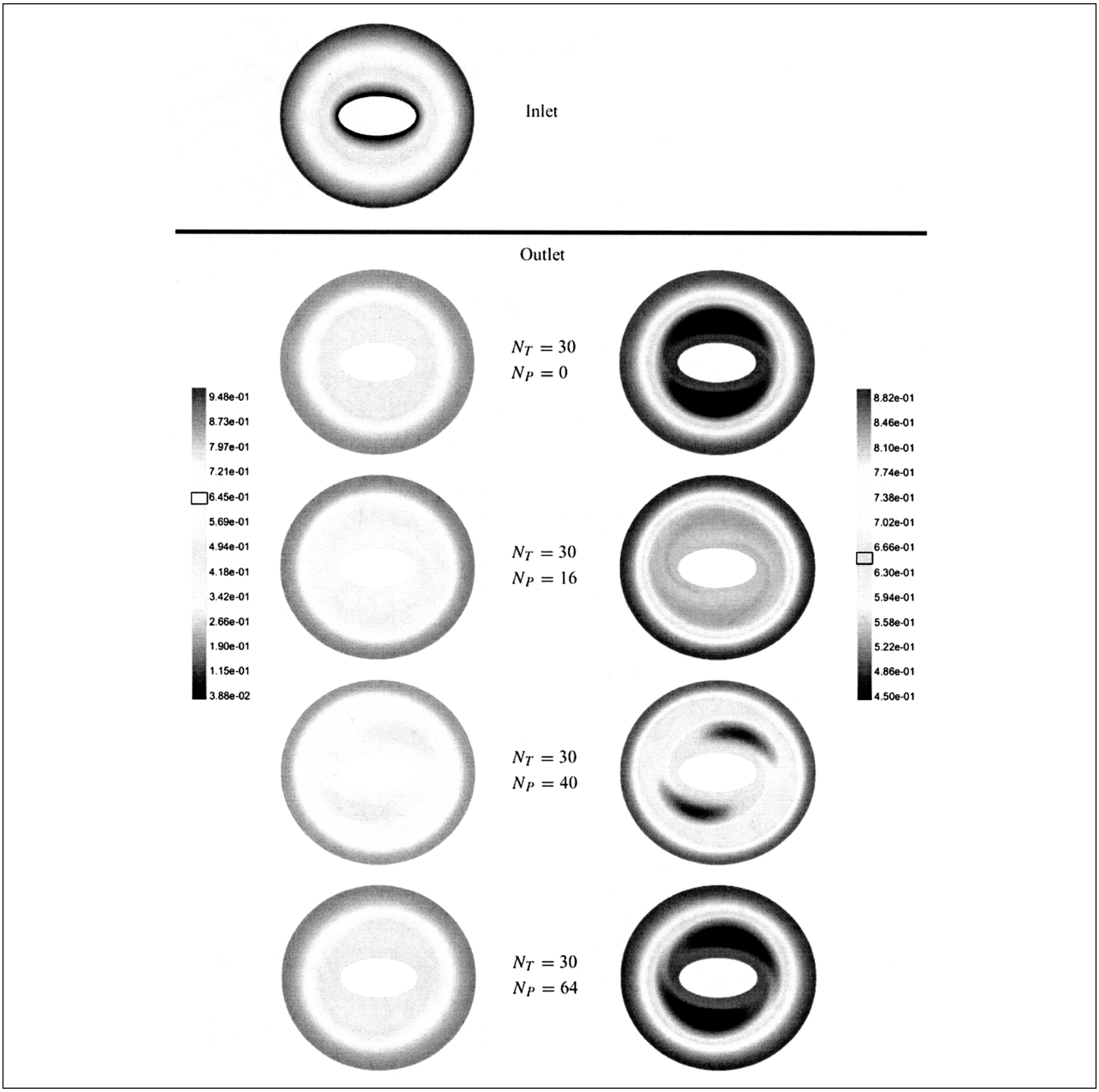

Figure 8. Outlet temperature distribution as a function of N_P for $N_T = 30$.

The geometric parameters and the velocity protocol are the same as in Figure 7. The values of N_P are: 0 (no modulation), 16, 40 (optimum modulation), and 64.

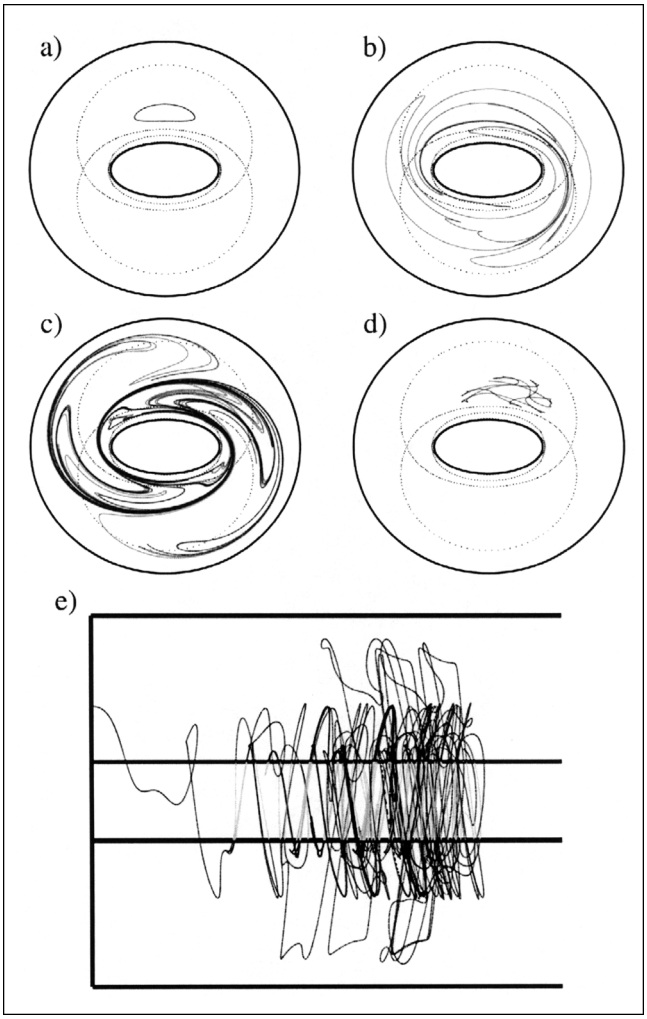

Figure 9. Streak lines plotted for the same conditions as in Figure 8.

Plots (a)–(d) show a cross-sectional view from the inlet of the streak-line for the corresponding value of N_P: (a) 0, (b) 16, (c) 40, (d) 64. The dotted lines represent the streamlines passing through the maximum and minimum saddle points. The bottom drawing (e) shows a lateral view of the streak line for the case $N_P = 40$.

For the same values of N_P and for $N_T = 30$, streak lines have been calculated and plotted on a plane. This is shown in Figure 9. For reference, the maximum and minimum saddle points (from which the potential mixing zone can be inferred) are also plotted. The same injection point (in the region of maximum gap) was used in all simulations. Notice that for the case giving the best mixing, that is, for $N_P = 40$, the streak line is very chaotic (Figure 9c). This is not the case for the other values of N_P. Furthermore, all along the mixer, the streak lines remain roughly in the potential mixing zone. The highly chaotic streak line obtained for $N_P = 40$ is shown as a function of the axial coordinate in Figure 9e.

Conclusions

An experimental setup used to study the chaotic 3-D laminar flow between confocal elliptic cylinders was built. This 2-D mixer geometry has been shown to possess certain advantages over the journal-bearing flow and could thus lead to more effective mixing. The experimental streak lines obtained were successfully compared to numerical calculations based on the analytical solution for the constant boundary-displacement case. This result is proof that both the experimental setup and the numerical solution of the dynamical system of three differential equations, with the pseudo-steady flow assumptions, are valid here. For the 3-D flow, particle trajectories stay in a region bounded by the vertical extension of the potential mixing zone. Although most tools used from the 2-D periodic flow are not useful here, the potential mixing zone seems to give a good estimate of regions where the trajectories will not go.

The effect of the modulation frequency was examined for the case of continuous, counter-rotation of the boundaries. For the class of periodic modulations considered here, the mixing rate depends on two dimensionless control parameters, N_T and N_P, which scale the cross-sectional stirring protocol with respect to the characteristic residence time. It is shown that for a given geometry and average axial velocity, there is an optimum modulation frequency for which the mixing process is optimized.

Acknowledgments

We acknowledge the financial support of FCT/MCT Praxis XXI/BD/18282/98, Praxis XXI/BCC/22223/99, and POCTI/EME/40057/2001 scholarships. This work was also partly supported by the Centre National de la Recherche Scientifique (CNRS) in the form of a 3-year scholarship for J. C. Leprévost.

Literature Cited

Acharya, N., M. Sen, and H. C. Chang, "Heat Transfer Enhancement in Coiled Tubes by Chaotic Mixing," *Int. J. Heat Mass Transfer*, **35**, 2475 (1992).

Aref, H., "Stirring by Chaotic Advection," *J. Fluid Mech.*, **143**, 1 (1984).

Aref, H., and S. Balachandar, "Chaotic Advection in a Stokes Flow," *Phys. Fluids*, **29**, 3515 (1986).

Barth, T. J., and D. Jespersen, "The Design and Application of Upwind Schemes on Unstructured Meshes," Tech. Rep. AIAA-89-0366, AIAA Aerospace Sciences Meeting, Reno, NV (1989).

Chaiken, J., R. Chevray, M. Tabor, and Q. M. Tan, "Experimental Study of Lagrangian Turbulence in a Stokes Flow," *Proc. Roy. Soc. Lond.*, **A408**, 165 (1986).

Franjione, J. G., C. W. Leong, and J. M. Ottino, "Symmetries within Chaos: A Route to Effective Mixing," *Phys. Fluids*, **A1**, 1772 (1989).

Gear, C. W., "The Simultaneous Numerical Solution of Differential-Algebraic Equations," *IEEE Trans. Circuit Theory*, **CT-18**, 89 (1971).

Horner, M., G. Metcalfe, S. Wiggins, and J. M. Ottino, "Transport Enhancement Mechanisms in Open Cavities," *J. Fluid Mech.*, **452**, 199 (2002).

Hutchinson, B. R., and G. D. Raithby, "A Multigrid Method Based on the Additive Correction Strategy," *Numer. Heat Transfer*, **9**, 511 (1986).

Jones, S. W., O.M. Thomas, and H. Aref, "Chaotic Advection by Laminar Flow in a Twisted Pipe," *J. Fluid Mech.*, **209**, 335 (1989).

Kaper, T. J., and S. Wiggins, "An Analytical Study of Transport in Stokes Flows Exhibiting Large-Scale Chaos in the Eccentric Journal Bearing," *J. Fluid Mech.*, **253**, 211 (1993).

Khakhar, D. V., J. G. Frangione, and J. M. Ottino, "A Case Study of Chaotic Mixing in Deterministic Flows: The Partitioned-Pipe Mixer," *Chem. Eng. Sci.*, **42**, 2909 (1987).

Kusch, H. A., and J. M. Ottino, "Experiments on Mixing in Continuous Chaotic Flows," *J. Fluid Mech.*, **236**, 319 (1992).

Leprévost, J. C., and E. Saatdjian, "Chaotic Heat Transfer in a Periodic Two-Dimensional Flow," *Phys. Fluids*, **10**, 2102 (1998).
Leprévost, J. C., "Mélange Laminaire dans les Écoulements Bidimensionnels Périodiques et Tridimensionnels Ouverts," Doctoral Thesis, Institut National Polytechnique de Lorraine, Vandoeuvre, France (2000).
Ottino, J. M., *The Kinematics of Mixing: Stretching, Chaos and Transport*, Cambridge Univ. Press, Cambridge (1989).
Peerhossaini, H., C. Castelain, and Y. Le Guer, "Heat Exchanger Design Based on Chaotic Advection," *Exp. Thermal Fluid Sci.*, **7**, 333 (1993).
Petzold, L., "Differential/Algebraic Equations are Not ODEs," *SIAM J. Sci. Stat. Comput.*, **3**, 367 (1982).
Poincaré, H., *Les Méthodes Nouvelles de la Mécanique Céleste*, Gauthier-Villars, Paris (1893).
Rodrigo, A. J. S., J. P. B. Mota, A. Lefèvre, and E. Saatdjian, "On the Optimization of Mixing Protocol in a Certain Class of 3-D Stokes Flows," *Phys. Fluids*. (2002).
Saatdjian, E., N. Midoux, and J. C. André, "On the Solution of Stokes Equations Between Confocal Ellipses," *Phys. Fluids*, **6**, 3833 (1994).
Saatdjian, E., N. Midoux, M. I. Chassaing, J. C. Leprévost, and J. C. André, "Chaotic Mixing and Heat Transfer Between Confocal Ellipses," *Phys. Fluids*, **8**, 677 (1996).
Swanson, P. D., and J. M. Ottino, "A Comparative Computational and Experimental Study of Chaotic Mixing in Viscous Fluids," *J. Fluid Mech.*, **213**, 227 (1990).

Manuscript received Aug. 1, 2002, revision received Feb. 25, 2003, and final revision received May 19, 2003.